International Journal of Computing and Digital Systems
ISSN (2210-142X)
Int. J. Com. Dig. Sys. 15, No.1 (Feb-24)

http://dx.doi.org/10.12785/ijcds/150135

Region Detection Technique Using Image Subtraction and Pixel Expansion Cue for Obstacle Detection System on Small – Sized UAV

Muhamad Wafi Abdul Aziz[1] and Muhammad Faiz Ramli[2]

[1]*Faculty of Mechanical Engineering, Universiti Tun Hussein Onn, Johor, Malaysia*
[2]*Department of Aeronautical Engineering, Universiti Tun Hussein Onn, Johor, Malaysia*
[3]*Research Centre for Unmanned Vehicle (ReCUV), Universiti Tun Hussein Onn, Johor, Malaysia*

Received 28 Mar. 2023, Revised 6 Jan. 2024, Accepted 21 Jan. 2024, Published 1 Feb. 2024

Abstract: This research paper is about method of detection of free region and obstacle region by combining image segmentation and frame subtraction method. The application will be further study to be used by Unmanned Aerial Vehicles (UAVs). This method intends to minimize the weight of UAV by avoiding heavy sensors. Objective of this research is to utilize the pixel expansion of object to find free region. K-means segmentation will be used to separate the interest area from the background. Then, segmented image frame will be subtracted and then divided into several grids and the amount of subtracted pixel that has been set into yellow and black color of each grid will be calculated with respect to distance given. The expansion of pixel will be detected as, the distance between image frame coming closer, number of obstacle pixel will be higher. The application of simple LIDAR that emits single ray to frontal obstacle will initiate the camera to capture image frame to be further analyze. Experiment was carried out in close environment with different cases and total of 100 images has been captured that consist of texture obstacle, texture-less obstacle, and multiple obstacles. The findings showed bearable results as the free region detection is 88.0% for texture obstacle and up to 84.0% of free region were successfully detected for texture-less obstacle. Due to lack of cues and texture in texture-less object, the algorithm had difficulties detecting the center of object that expands in static form.

Keywords: Image segmentation, Obstacle detection, Monocular camera, Pixel expansion, K-means, Free region detection

1. INTRODUCTION

The nature of UAVs that can be controlled remotely and flown at different range of altitude and distances is the key point of why it is preferable by human to execute any high risk and time-consuming inspection task [1], facilitates delivery [2], help save lives [3] , variety of military applications[4], and excellent in recording videos and capturing images [5]. To perform the mentioned tasks, a safe path needs to be established to avoid any upcoming obstacles that become the main factor that hinders the movement of the UAV. Detection of obstacles is crucial as any collision may lead to hardware damage or fatality as the UAV will be in airborne state while operating. Detection of obstacle can be executed by using several sensors that can be categorized as range-based sensor [6][7] and vision-based sensor [8][9][10]. Range-based sensor will directly calculate and produce the exact distance of the obstacle from the UAV, for example, ultrasonic sensor (US) [11] , light detection and ranging (LIDAR) [12][13] , radar [6], Kinect [14], and sonar sensor[15]. The benefits of range-based sensor are affordable and great in estimating the detected obstacle's distance, but lacking in information on the detected obstacle's position or bearing in the surrounding environment. Range – sensors are large in size, heavy and not compatible with micro-UAV that have low weight and price[16], or those that consume a lot of energy [17] and sensitive to the atmosphere [18]. Besides, infrared and sonar sensors detect object only within one meter range [2]. Vision based sensor consists of stereo camera – based obstacle detection [19][20][21] and monocular camera – based obstacle detection sensor[22][23][24][25]. Camera sensor is a passive sensor [26] that have poor object distance detection but, contain huge amount of information that can be further analyze in terms features of edges [27][28], point[29] and grayscale values [30] to detect object. Robust application of UAV is challenging especially for micro-UAV as its capability is limited within Size, Weight, and Power (SWaP) [29]. Therefore, implementation of vision – based sensor such lightweight on-board camera with low power consumption will be the solution for this challenge.

E-mail address: muhdwafi09@gmail.com, faizr@uthm.edu.my

In this paper a method of image frame subtraction and pixel expansion is proposed to detect obstacle region and a free region. Appearance based approach will be implemented in this research where image will be separated into uniform background and foreground that contain obstacle. The hypothesis in this research is that when sequence of images taken with respect to forward movement of UAV, object size from the second image frame will be larger when compared to the initial image frame of the same object as shown in Fig 1. This paper will propose a method to classify two different regions from subtracted image frame that will be known as free region and obstacle region. Only frontal obstacles will be included in this research as the movement of UAV is assumed to be only on forward direction.

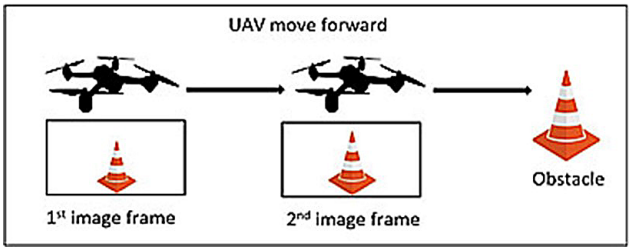

Figure 1. Pixel of obstacle increases as UAV moves closer to the obstacle

To further understand the concept of pixel expansion, see Fig 2 (a), the initial image has a total of 29 red pixel counts covered over the total of 156 pixel counts (width ×height)=(13pixels ×12pixels).However, as shown in Fig 2 (b), when the object is closer to the camera, the number of red pixels covered increases to 48 pixel counts of 156 pixels. Therefore, with subtraction of pixel counts of second image and first image, the remaining excess pixel is 14 pixels counts that will represent as pixel expansion.

This research will propose a new method for obstacle detection and the main contributions are:

- Develop a method of region classification by classifying obstacle region and a free obstacle region.
- Implement a new expansion-based approach that calculates the increasing pixel number of subtracted image frame.

The research questions can be referred from these queries: first, does the amount of specific pixel color of the object inside image frame will increase as the UAV moves closer to the object? Secondly, will multiple objects that have different distance from UAV have the same pattern of pixel expansion? Finally, how might the emergence of a poorly textured obstruction or a texture-less obstruction in the surroundings be identified and detected by a vision-based sensor? The remaining of the article is constructed as follows: section 2 presents previous works related to obstacle detection that involve range – based sensor and monocular vision – based sensor and its disadvantages. The

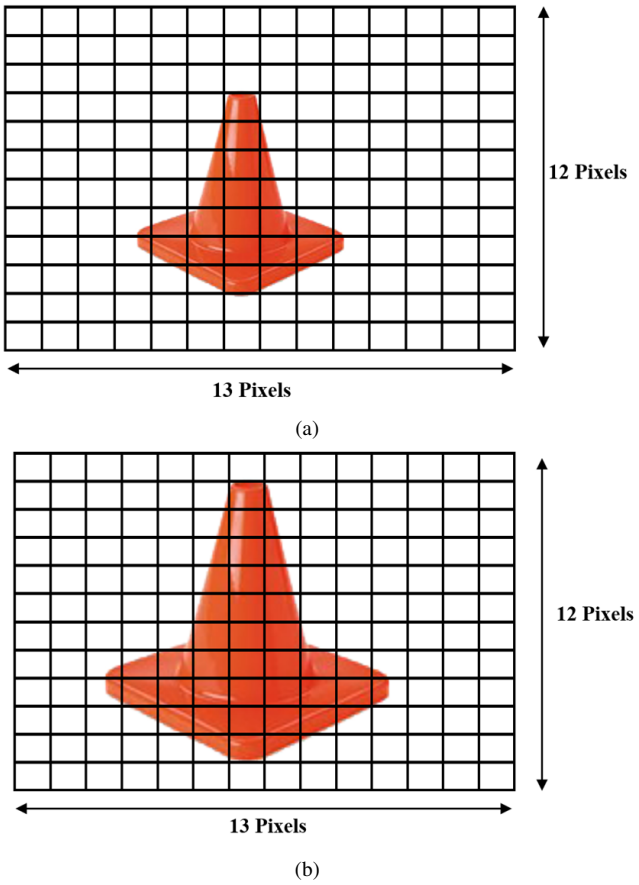

Figure 2. Comparison of pixel expansion between:(a). Initial Image Frame (b). Expansion Image Frame

introduction of proposed method, framework is composed in section 3 under methodology. The experiment of proposed method, related hardware, discussion, and result include in Section 4. Lastly, section 5 conclusion and future recommendation of research and recommendation.

2. RELATED WORKS

Monocular cameras are suitable for compact UAV which makes it preferable to be used as it is also computationally inexpensive. The techniques of obstacle detection of monocular camera mostly depend on the cues of the object in term of color [31], shape [32], corners[33], and edges [34]. This cue information is then further utilized into specific method such as pixel growth-based method [29], depth-based method[10], and image movement -based method [34].

A. Pixel Growth-based method

As objects become nearer, the size of the object will be larger compared to previous situations, same as human perception. This method will utilize the object expansion rate between consecutive images. In [35], applied the SURF algorithm's properties to find the initial locations of obstacles of various sizes. Despite having simple computations, this approach might fail because of slow reaction time to

obstacles. Another research in [9] employed edge motion in two subsequent frames to detect incoming obstructions. The object enlarges if its edge moves outwards (relative to its center in subsequent frames) and is applied to fixed and mobile robots. When the background is uniform, both stationery and mobile robots can use this method. This strategy only works for static items and is not suitable for complex backgrounds. Researcher in [32] use compact UAV as platform to test obstacle detection method by implementing SURF method to detect some primary patterns as obstacles. Hence only specific obstacles can be detected, and the detection of obstacles is not robust. [16] compared and extracted points from subsequent frames using SIFT method [36]. He then created a convex hull with respect to the matching points. The points were regarded as obstacle points if the change in their SIFT scale values and the convex hull area exceeded a certain threshold.

B. Depth-based method

Information taken for dept-based method are from images captured by single camera. To obtain depth, motion stereo or deep learning techniques can be implemented. In the former, two cameras are mounted on the sides of the robot, and two repeated photos are taken. Although only one camera was used to capture these images, they may be seen as a pair of stereo images that can extract the estimation depth of object points. A matching point will be implemented between the images and calculations of depth estimation will be used. In paper [10], use four fisheye cameras and motion stereo to produce depth maps and obstacles are denote as any object on the ground. However, this method cannot detect moving objects and is highly computational. Next,[31] implemented Inertial Measurement Unit (IMU) with fisheye camera in wide field of view (FOV) and depth estimation was based on keyframe for Micro UAV. Unfortunately, depth method cannot run as the MAV hovering and camera produce low image quality. In terms of artificial neural networks and deep learning, [37] applied a CNN and four single fisheye cameras on self-driving cars to determine the depth in every direction. However, this research requires further data training. Method [38] offers fast obstacle detection by producing the latest CNN framework that use image features through fine-tuning the VGG19 network to estimate depth and detect obstacles. Moreover, multi-hidden-layer neural networks that can predict the distance called (DisNet) were introduced by [39].

C. Motion-based method

In [40], a unique approach utilizes motion characteristics to identify obstacles apart from shadows and traffic signs. To achieve real-time obstacle recognition, they only relied on corners and Scale Invariant Feature Transform (SIFT) features, rather than all pixels. If the failure rate of features matching is high, such an algorithm may not succeed. Commonly, most motion-based methods primarily use optical flow as their source of data. Without a map of the surrounding area, method [41] kept a mobile robot from colliding with objects. However, the position of looking downward camera may not suitable if the obstacle is higher than camera lens. To assist persons with visual impairments in navigating indoor spaces, [34] [40] employed two consecutive frames to estimate the optical flow for obstacle identification on smartphones. They computed the separation between two successive frames using a context-aware combination data approach. However, this method detects some incorrect points in lamps, floors, and reflective surfaces. Method in [42], validate Speeded-up Robust Features (SURF) [43] point detector as locations obstacles, by using Support Vector Machine (SVM). In this study, the data needed to train the SVM were extracted using a dense optical flow technique. Then, they applied obstacle points and measures related to the spatial weighted saliency map to locate the obstacles. Their research method is applicable to mobile robots with cameras mounted at low elevations. Therefore, using it on UAVs that often fly at high altitudes would not be practical. The summary of past researchers is shown in Table I.

3. METHODOLOGY

In this section, the method for free region and obstacle region classification will be shown and further explained. The proposed method will be divided into three sections: Attain and construct image data, Image processing, and Pixel expansion and region detection. With the help of simple LIDAR, the monocular camera sensor will be activated to capture and collect input image data after the emitted single ray of LIDAR hits frontal obstacle. This process will

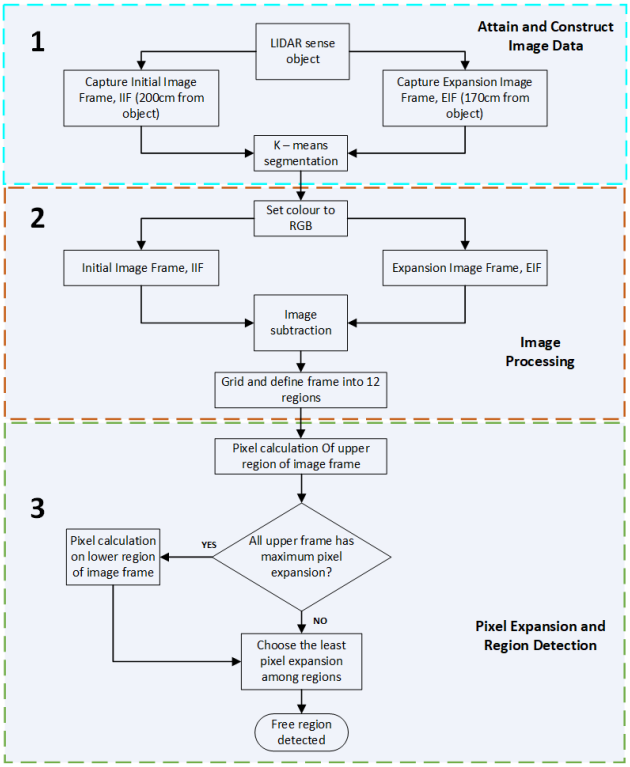

Figure 3. Framework of proposed method

TABLE I. SUMMARY OF PREVIOUS WORKS

Method	Disadvantages
Pixel Growth-based method	
SURF algorithm[31]	Slow reaction time to obstacle makes the calculation fail
Edge detection [9]	Not suitable for complex background
SURF method [32]	Cannot detect obstacles with different pattern.
Key points scale ratio and convex hull area ratio [16]	Robot have limited maneuverability in complex situation
Depth-based method	
4 fisheye camera and depth motion [10]	Highly computational
Fisheye camera and Inertial Measurement Unit (IMU)[34]	Low image quality (not accurate)
Image Features via fine-tuning the VGG19 network [36]	Appropriate data training needed
Hidden-Layer Neural Network (DisNet) [37]	Need adequate initial training
Motion-based method	
Scale Invariant Feature Transform (SIFT) [38]	High number of mismatch features.
Optical flow [39]	Downward looking camera (limited obstacle detection)
Optical flow and point track [40]	Incorrect detection of some points on lamps, floors, and reflective surfaces
Optical Flow data for Support Vector Machine (SVM) [41]	Not suitable for UAV

be done twice at the initial distance of 200cm and 170cm from the camera sensor to the obstacle. The input image data will be further gone through image processing section where K – means clustering occurs to simplify the input data of random pixels colors into only 3 types of pixel colors of both images.Then, the images frame at 170cm will be subtracted with the image frame of 200cm and further color simplification of only 2 types of pixels will be done to detect between pixel expansion and static pixel. Later, to facilitate the method, the subtracted image frame will be segmentized by grided into 12 region area that will be define as true obstacle region and indecisive region. Then, the least amount of pixel expansion which can be concluded as the free region area will be selected among the region area. The framework is shown in Fig 3.

4. ATTAIN AND CONSTRUCT IMAGE DATA

The usage of LIDAR in this research is to trigger the camera to capture image frame. The distance is to be set 200cm from the UAV If any obstacle detected within the range, the camera would start capture the first image frame. To obtain a set of pixel expansion data for the purpose of proving this research method, the camera will capture the image every 10cm forward movement by the UAV that will be supervised by LIDAR. The set of image frames taken with respect of forward distance is 200cm, 190cm, 180cm, 170cm, 160cm and 150cm to produce a trend of pixel expansion with respect of decreasing distance towards the obstacle. On other hand, for the purpose of finding free region and obstacle region, experiment will be conducted by the image captured with respect of distance of only image frame at 200cm Initial Image Frame (IIF) and 170cm Expansion Image Frame (EIF) that will be further process into the algorithm as shown in Fig 4 that will be further explain in section 4.

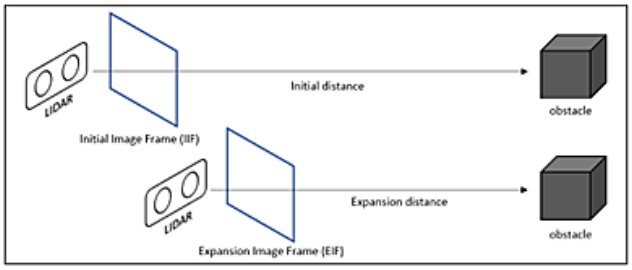

Figure 4. LIDAR detection

5. IMAGE PROCESSING

A. K - means Segmentation

Application of image segmentation will be complex when the image is classified as over-segmented, and all the data are randomly mixed up without any grouping and not optimized therefore difficult to analyze the data. In image processing, segmentation of the image can be the solution for this problem and there are several methods for segmentation technique such as edge method [44], threshold method [45], cluster method [46],[47] and neural network-based method[48]. Clustering based method is the most powerful for image segmentation and there were branches of clustering method such as K–means clustering [49][50][51][52][53], Fuzzy C–means clustering [54], [55], mountain clustering [56] and subtractive clustering method[53]. Generally, clustering is a grouping approach that uses a similarity metric to place comparable things in the same group and dissimilar ones in distinct groupings. K–means clustering is an unsupervised machine learning

approach that divides N observations into K clusters, with each observation assigned to the cluster with the closest mean. A cluster is a collection of data items that have been aggregated together due to commonalities. Clusters in this case are various pixel colors used for image segmentation. The usage of K-means segmentation is selected because it is easier to use and performs computations more quickly compared to hierarchical clustering and it may also be used with a lot of different variables[53] . The input image as shown in Fig 5 (a) will be classified into 3 colors that choose K = 3 which are red, green, and blue to simplify the complex mixed pixel data as shown in Fig 5 (b).

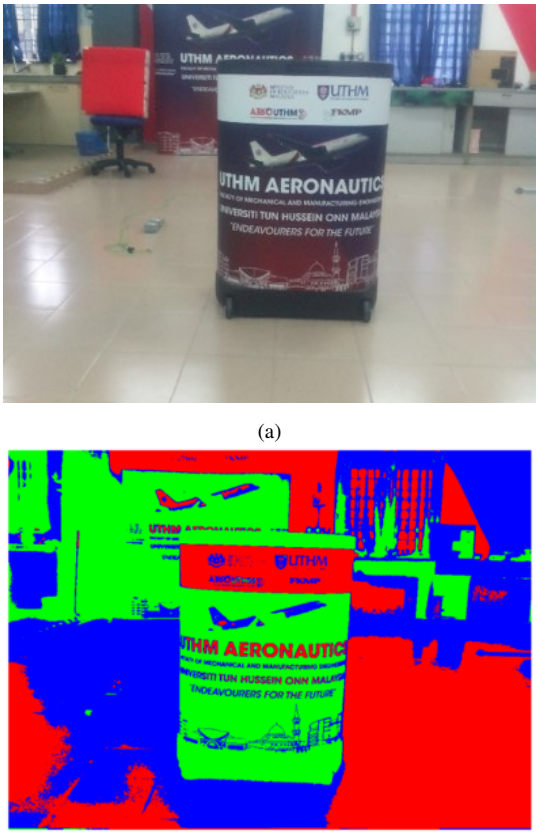

(a)

(b)

Figure 5. (a) Input image data, (b) Image data after applying K – means clustering

The K-means algorithm comprises two distinct stages. The K centroid is calculated in the first phase, and then in the second phase, each point is taken to the cluster with the centroid that is closest to it. The steps of applying K-means segmentation are as below:

1) Randomly, initialize K centroids.
2) Based on its color value, assign each pixel in the picture to the nearest centroid. The Euclidean distance formula may be used for this step are as below:

$$d(x,y) = \sqrt{\sum_{i=1}^{n}(x_i - y_i)^2}$$

where,
x, y = two points in Euclidean n-space
$x_i - y_i$ = Euclidean vectors, beginning at the space's origin(initial point)
n = n-space The color values of two pixels are defined as x and y and their corresponding RGB values are x1, x2, x3, and y1, y2, y3.

3) Calculate each cluster's new centroid.
$$c_k = \frac{1}{k} \sum_{y \in c_k} \sum_{x \in c_k} p(x,y)$$

4) Steps 2 and 3 should be repeated until the centroids no longer change or the maximum number of iterations is achieved.

5) Once the centroids have converged assign each pixel in the picture to its nearest centroid and color it with the color of the centroid. This will result in a picture with K distinct areas, each represented by a different color.

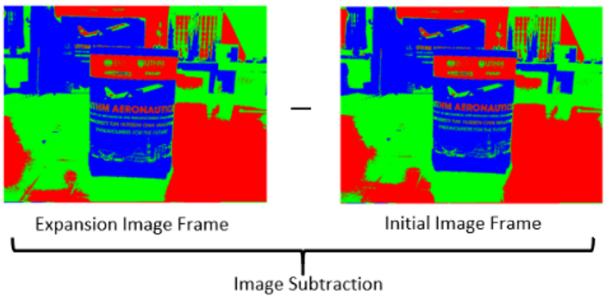

(a)

(b)

Figure 6. (a) Image subtraction process, (b) Result of subtracted images

Despite all its benefits, the (Random Initialization Trap)—a failure caused by the random selection of centroids can cause K-Means to occasionally fail. K-Means initialization is used to counter the problem by which, first centroid is chosen at random, and the likelihood of the following point is determined by the distance of the previous one; the

more apart the points are, the higher the possibility that it will be chosen. The probability of each point depends on its distance from the centroid that is closest to it once we have two centroids

B. Image Subtraction

After applying K-means clustering, the image will be further processed into subtraction of pixel as shown in Fig 6 (a). Generally, the pixel subtraction operation takes two pictures as input and outputs a third image with pixel values that are the first images minus the second image's corresponding pixel values such in Fig 6 (b). Some application of image subtraction is to locate differences between two photos or to level out uneven areas of an image, such when half of it has a shadow on it by taking a single picture as input and just take out a certain amount from each pixel. Instead of the obvious signed output, some implementations of the operation only give the absolute difference between the values of the pixels. The aim of image subtraction in this research is to calculate the expansion of pixel by seeing the increasing in object compared from first frame distance with second frame distance. From Fig 6 (b), the subtracted image contains excess colors of (R, G, B) result from pixel expansion and black region is where no expansion of pixel occurs. From the subtracted image, we can understand that any forward movement that makes the second frame object larger, when being subtracted by first frame, there will be a boundary of which the excess pixel result from the forward movement. The red, blue, and green components are simply subtracted one from the other to create the output value since in this research we have limit the K value to 3 for RGB.It is simple to accomplish the subtraction of two images in a single pass. Let's define IF as image frame and (x,y) as the pixel's coordinate The values of the output pixels come from:

$$\mathrm{IF}_{subtract}(x,y) = IF_{EIF}(x,y) - IF_{IIF}(x,y)$$

As an alternative, if the operator calculates the absolute differences between the two input photos, then:

$$\mathrm{IF}_{subtract} = |IF_{EIF}(x,y) - IF_{IIF}(x,y)|$$

where,
IF = Image Frame
x = horizontal coordinate of pixel
y = vertical coordinate of pixel

In Figure 6. (a), the red, green, and blue colors are all mixed therefore difficult to extract the data from the image frame. Hence, by define P as pixel value,

$$\mathrm{IF}_{subtract} \begin{cases} (255,0,0)_R \\ (0,255,0)_G \\ (0,0,255)_B \end{cases}$$

then,

$$\mathrm{IF}_{subtract} \begin{cases} ((255,255,0)_{PY} \\ (0,0,0)_{PB} \end{cases}$$

where,
Py = Pixel expansion - yellow
Pb = No Pixel expansion(static) - black

Therefore, only yellow colors will be defined as the excess obstacle Pyellow while Pblack the black is the static region as shown in Fig 7 (a).

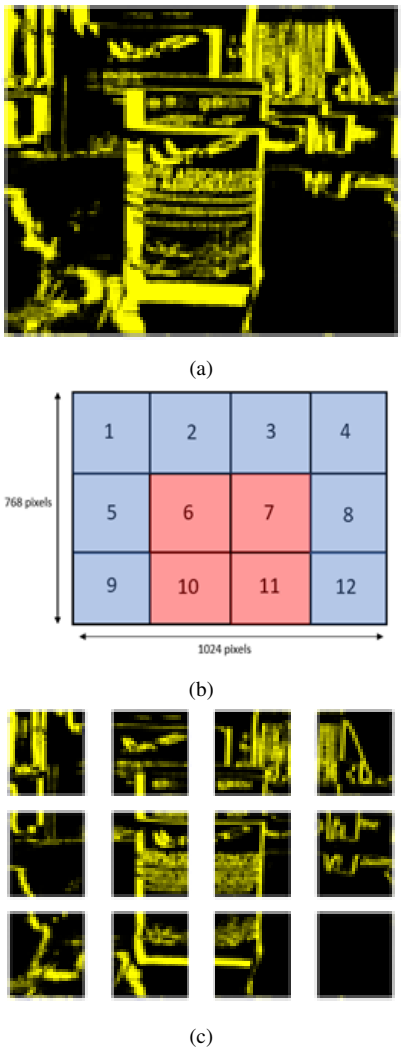

(a)

(b)

(c)

Figure 7. (a) Image subtraction process, (b) Result of subtracted images, (c) Subtracted image Grid

C. Define Grid

The subtracted image frame will be divided into 12 areas. The dimensions of our image frame are (768x1024) height and width. The objective of implementing grid is to simplify the filtering of obstacle region and the free region which is inside the corresponding 12 areas of boxes as shown in Fig 7 (b) and (c). Next, the grid will be defined

between true obstacle area 6, 7, 10 and 11 (Red region) and indecisive area 1, 2, 3, 4, 5, 8, 9, 12. For flying UAV, it is better to fly away from the ground to avoid any direct hit with ground objects therefore we filter again the indecisive area to prioritize the upper area region first to detect the free obstacle region area 1, 2, 3, 4, 5, and 8 (Blue region). If there is no exact free region, the program will calculate the last two lower regions which is area 9 and 12. The reason why there is red region or true obstacle region is that region inside the boundary of LIDAR detection is confirmed that there will be an object inside the boxes when LIDAR emits its rays inside the red region.

6. PIXEL EXPANSION AND REGION DETECTION

When the camera moves forward, the object inside the image will become larger thus, the pixel also will increase. Therefore, the proposed pixel expansion queue will take place. Calculation of the pixel expansion is straight forward from the pixel amount of the individual colors. From Fig 7, the calculation of pixel expansion is based on black and yellow colors with respect to the total height times width of the frame. By using python programming, we can calculate the amount of pixel expansion which in this case we will define yellow as the object expansion and black is where there is zero expansion and background. The calculation of the total yellow pixel will take place of each indecisive region and the lowest amount of yellow pixel will be selected and confirmed as the free region with respect of the total pixel in the region.

$$\sum IF_{subtract} = \sum P_Y + \sum P_B$$

Then, define R as grided area region and n as the grid number,

$$R_{Area\ n+1} = \sum P_Y$$

Free region=$R_{Area\ n}$(*with least* P_Y *amount*)

amsmath

From combination of Py and Pb that produced subtracted image IFsubtract, the program will calculate the least amount of pixel Py from the Rarea n+1. Then, the free region area will be selected from the least amount of yellow pixel number with respect to the grided region area. To answer the query in section 1 (does the amount of specific pixel colors of the object inside image frame will increase as the UAV move closer to the object?), and (, will multiple object that have different distance from UAV will have the same pattern of pixel expansion?), consider the graph shown in Fig 8 (b) to examine the behavior of the pixel expansion cue. The image taken from Fig 8 (a) to form a graph in Fig 8 (b) and the data of yellow pixel (object expansion) are shown in Table II shows that pixel expansion and distance have an inversely proportionate connection and the nearer the UAV to the object, the greater the pixel expansion will be[7][34].

From the graph shown in Fig 8 (a), the main obstacle is the object inside the true obstacle area 6, 7, 10 and 11 as shown in Fig 7 (b). Side obstacles are located inside the indecisive area 1, 2, 3, 4, 5, 8. It is clearly shown that the expansion rate compared to the main obstacle is faster and larger compared to the side obstacle. From Table II, the data shows object pixel expands simultaneously but the side obstacle has lower number of pixel expansion compared to the main obstacle. This is because of the difference in distance between the object and the camera sensor. Thus, the question in section 1 (will multiple object that have different distance from UAV will have the same pattern of pixel expansion?) has been answered.

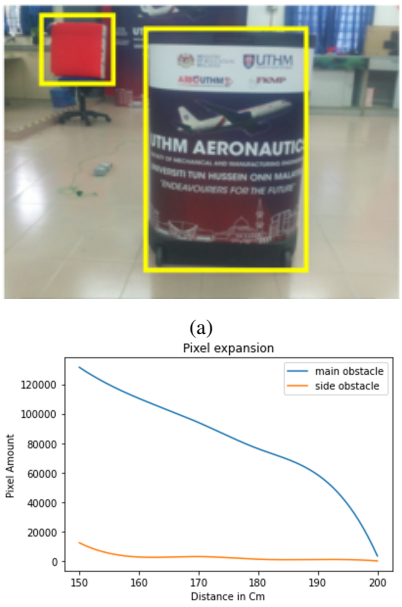

(a)

(b)

Figure 8. (a) Main obstacle at centre and side obstacle at the left of main obstacle, (b) Graph of Comparison of Pixel Expansion

TABLE II. Data of Pixel Expansion for Main and Side Obstacles

Distance (cm)	Pixel Main	Pixel Side
200	10078	911
190	63676	3246
180	83441	3553
170	104330	9468
160	122416	12280
150	150404	28984

7. EXPERIMENT RESULT AND DISCUSSION

The hardware involved is range sensor, TF Mini – Micro LIDAR Module, Fig 9 (a) with 8-meter range capability of object detection. This sensor was selected because it is weightless and affordable. The usage of LIDAR in this research is to trigger the camera sensor to capture the image after obstacle is detected at certain range. As the free region classification is limited to frontal area of the UAV, we only use single ray LIDAR that emits single ray

directed to one point forward. Raspberry Pi 4 Model B 8GB Quad core Cortex-A72 (ARM v8) 64-bit, Fig 9 (b) is the microcomputer used for programming execution and communication between LIDAR sensor also camera sensor. Finally, Raspberry Pi Camera Rev 1.3 Fig 9 (c) was selected to capture the frontal image and acquire data for image processing.

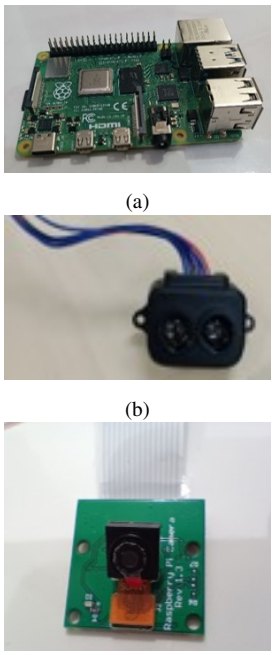

(a) (b) (c)

Figure 9. (a) Raspberry Pi 4, (b) LIDAR, (c) Pi Camera

Several obstacle detection and avoidance tests have been conducted with different object textures used to assess the effectiveness and capabilities of the proposed system. The proposed experiment and method were executed in an indoor environment. The experiment area is 10 meters length and 8 meters width. The experiment setup will be categorized into detecting texture obstacles and texture-less obstacles. Cases 1 to 5 below will be the arrangement of the obstacles for free region detection. The case will be separated into texture obstacle and texture-less obstacle.

- Case 1: Only a single obstacle detected in front of the UAV.
- Case 2: Main obstacle and side left obstacle with same distance.
- Case 3: Main obstacle and side left obstacle with 100 cm distance behind the main obstacle.
- Case 4: Main obstacle and side right obstacle with 100 cm distance behind the main obstacle.
- Case 5: Main obstacle and right obstacle with same distance.

The experiment is performed in 5 different cases (multiple obstacle or single obstacle) with fix distance of Initial Image Frame (IIF = 200cm) and Expansion Image Frame (EIF = 170cm) and the percentage of success rate were calculated over the success of free region detection of 5 cases that has been repeated for 5 times each in order to verify the robustness of proposed method. The experimental setup and condition are shown in Fig 10. Texture object is anybody of the object that has discontinuity or sharp change of the pixel such as corners in the object's body texture. Texture – less is any object that has plain body and doesn't have any sharp changes or discontinuity in pixel inside the body such as wall or plain boxes.

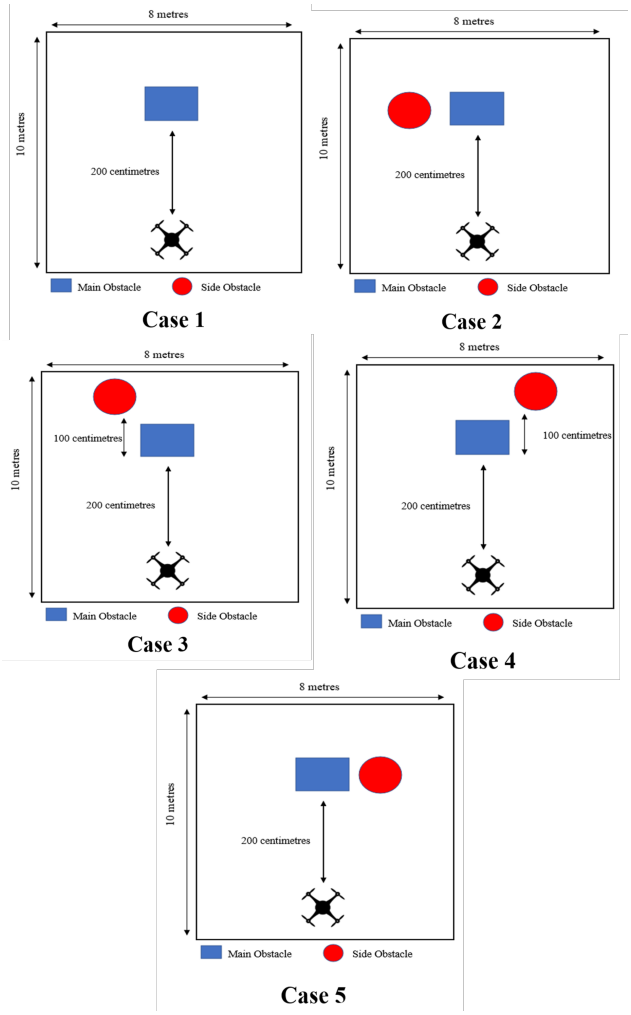

Figure 10. . Different cases of obstacle placement to test the robustness of proposed

From Table III and IV, the initial distance of 200cm from the object has been selected as the avoidance of the obstacle will not be done too early before the obstacle. Expansion image frame EIF or second image frame captured selected is 170cm so that the pixel expansion is not too small to detect the expansion difference between foreground object

TABLE III. Region Detection For Texture Obstacles

Case	Texture Obstacle		Free Region Detection	Success Rate
	Main	**Side**		
Case 1	Yes	No	5/5	100%
Case 2	Yes	L	2/5	40%
Case 3	Yes	L 100cm	5/5	100%
Case 4	Yes	R 100cm	5/5	100%
Case 5	Yes	R	5/5	100%
Computational time	**227.84ms**		Overall Success Rate	**88.0%**

TABLE IV. Region Detection For Texture - less Obstacles

Case	Texture Obstacle		Free Region Detection	Success Rate
	Main	**Side**		
Case 1	Yes	No	5/5	100%
Case 2	Yes	L	2/5	40%
Case 3	Yes	L 100cm	5/5	100%
Case 4	Yes	R 100cm	4/5	80%
Case 5	Yes	R	5/5	100%
Computational time	**216.4ms**		Overall Success Rate	**84.0%**

and background object[8]. Choosing a small gap of distance (example IIF = 200cm, EIF = 190cm) between the initial image frame and expansion image frame will increase the computational time as the program needs to execute the code in a short period of time.

In Table III, the overall success rate for obstacles with texture is 88.0%. Run in the table means the attempt of coding been executed. Only object in case 2 not fully detected by the proposed method as shown in Fig 12 and 13. For case 2, only 2 out of 5 images can detect the free region in the first image set and the last set of images that consist of free region in region 4 and region 1 of the grid image frame. Only 1 set of images can be detected by the method for free region in area region of region 4. The failure of the method to detect free region due to the expansion image is shifted to the right or left therefore the expansion of the object is not uniform thus the calculation of pixel expansion is less accurate. However, only partial obstacles are included inside the free region area as shown in red circle in Fig 12 and Fig 13. Thus, there are still some parts in the selected region that are not covered by the obstacle that can be tackled in future research. In Table IV free region detection for texture-less object, proposed method failed to detect free region of some set of images in case 2 with only 20% of success rate and case 3, 20% success rate and case 4 with 80% of success rate as shown in Fig 14 and Fig 15.

See Fig 14, 15 and 16, where part of the obstacle is included inside the free region frame as the method detects that region with less total pixel expansion due to. Comparing the overall success rate of free region detection, obstacles with texture produce higher success rate (88.0%) compared to the texture-less obstacle (84.0%). The difference between success percentage due to texture-less obstacle did not have any cues inside the body of the obstacle thus the expansion inside the boundary of obstacle's body to be said as zero or expand in static form. Generally, the limitation and weakness of proposed method to detect free region area are as below:

1) The distance between the initial image frame and expansion image frame is small thus difference in pixel expansion between foreground object and background object cannot be differentiate.
2) Expansion image frame capture has been shifted to the left or right direction due to error taking second image frame (sensitive to movement).
3) Only a small part of boundary of the obstacle included inside free region area as there is no cue of expansion inside the end of the boundary of obstacle.

To overcome the above limitations, the distance between the initial image frame and expansion image frame must be increased. Next, the movement of forward direction of camera must uniform. Lastly, application of distance transform can be applied to avoid zero-pixel expansion inside the end of the boundary of obstacle. From Table III and Table IV, compared to previous works [57] used SIFT and Multi-scale Oriented-Patches have computational time of (577ms), the proposed method only need (216.64ms) for texture-less and (227.84ms) for texture obstacles to detect free region. [8] use SURF size expansion characteristic and ratio of size changes that detect texture-less obstacle 90cm behind main obstacle with success rate of 20% compared to proposed method that able to detect side obstacle with distance of 100cm with success rate of 84%.

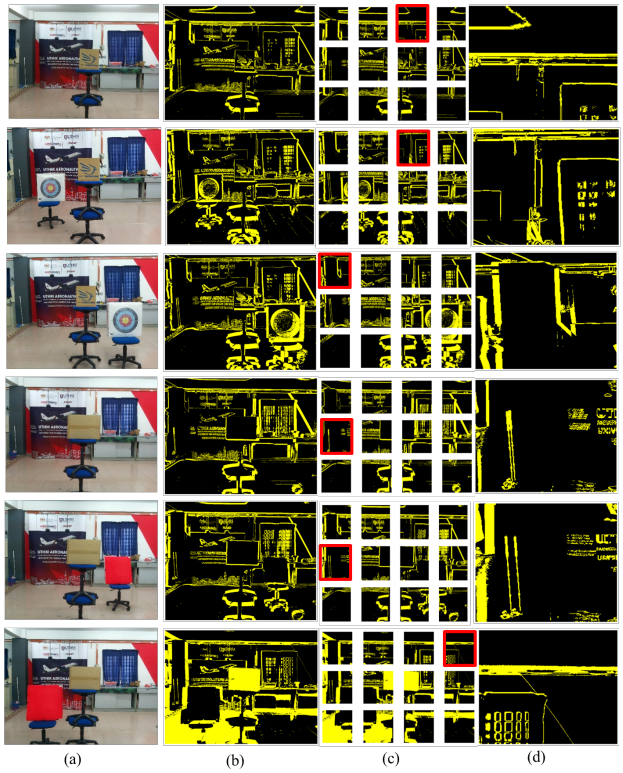

Figure 11. Sample of random image taken from experiment. a) Input image b) Subtracted image c) Applying grid , d) Results of free region

Figure 12. Obstacle in Case 2 that fail to detect free region.

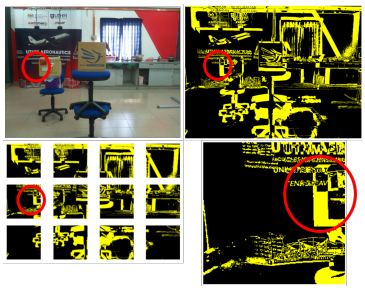

Figure 13. Obstacle in Case 3 that fail to detect free region.

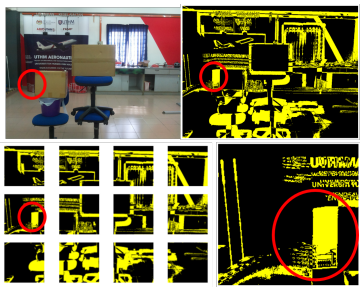

Figure 14. Texture less obstacle fail detect free region in Case 2.

8. CONCLUSION AND FUTURE IMPROVEMENT

The application of image subtraction and pixel expansion for region detection of monocular cameras has been proposed. To ensure the method works appropriately, we combine the simple LIDAR to set range of UAV from the obstacle which is 200cm in this research for the lightweight monocular to activate and capture the initial image frame IIF. This method successfully detected free regions that contain the minimum pixel expansion among 12 regions. This method is direct and simple and able to provide satisfying region classification. This research also uses multiple obstacles to prove the expansion rate by comparing both obstacle and the selection of free region is based on the least amount of pixel expansion among indecisive area 1, 2, 3, 4, 5, 8, 9, 12. This research has shown and answer the query in the first section that the amount of specific pixel color of the object inside image frame will increase as the UAV move closer to the object Secondly, multiple object that have different distance from UAV will have same pattern of expansion but the side obstacle that further from main obstacle and camera sensor will produce slower expansion rate, as shown in Fig 7(b). Third, emergence of poorly textured obstruction result in difficulties of the texture-less obstruction to be detect and analyze by the proposed method as the expansion of pixel near to static at the center of the obstacle Finally, range-based sensor can be integrated with vision-based sensor to strengthen the obstacle detection process and cover each other weakness by initiate the camera sensor to capture image data. However, there are some poor sides of this method that can be further study to make some improvement listed as below:

- The camera must move straight forward direction without any disturbance from any direction.
- There is an empty area inside the object (black region) after being subtracted that has no expansion even if it is object.

This method will be further applied to micro-UAV for region detection and obstacle avoidance to generate safe path of the micro-UAV. In future work, we will improve the weakness of the proposed method and increase the rate of success or precision of free region detection by perform further experimentation with various scenarios in complicated environments. Apart from obstacle detection, image processing methods are also being implemented in other sectors[58][59][60]. The proposed method can be beneficial

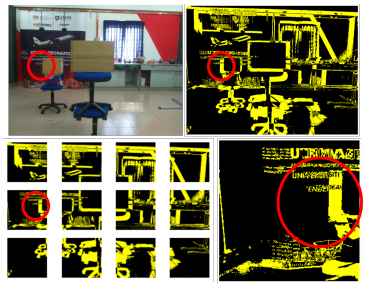

Figure 15. Texture less obstacle fail detect free region in Case 3.

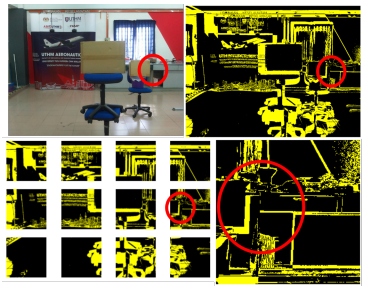

Figure 16. Texture less obstacle fail detect free region in Case 4

for the development of autonomous vehicles, surveillance systems, robotics, industrial automation, and healthcare. In further research semantic segmentation method would be implement into the proposed obstacle detection algorithm to increase the frontal and multiple object detection's reliability of micro-UAV.

9. ACKNOWLEDGEMENT

This research was supported by Universiti Tun Hussein Onn Malaysia (UTHM) through GPPS (vot Q210) and Tier 1 (vot H920).

REFERENCES

[1] C. Eschmann, C. M. Kuo, C. H. Kuo, and C. Boller, "Unmanned aircraft systems for remote building inspection and monitoring," vol. 2, 2012.

[2] Z. Zhang, M. Xiong, and H. Xiong, "Monocular depth estimation for uav obstacle avoidance." Institute of Electrical and Electronics Engineers Inc., 12 2019, pp. 43–47.

[3] A. G. Arenzana, J. J. E. Macias, and P. Angeloudis, "Design of hospital delivery networks using unmanned aerial vehicles," *Transportation Research Record*, vol. 2674, 2020.

[4] M. Calderón, W. G. Aguilar, and D. Merizalde, "Visual-based real-time detection using neural networks and micro-uavs for military operations," vol. 181, 2020.

[5] F. Outay, H. A. Mengash, and M. Adnan, "Applications of unmanned aerial vehicle (uav) in road safety, traffic and highway infrastructure management: Recent advances and challenges," *Transportation Research Part A: Policy and Practice*, vol. 141, 2020.

[6] C. Giannì, M. Balsi, S. Esposito, and P. Fallavollita, "Obstacle detection system involving fusion of multiple sensor technologies," vol. 42, 2017.

[7] M. F. Ramli and S. S. Shamsudin, "Obstacle detection technique to solve poor texture appearance of the obstacle by categorising image's region using cues from expansion of feature points for small uav," *International Journal of Computational Vision and Robotics*, vol. 1, 2022.

[8] M. F. B. Ramli, S. S. Shamsudin, and A. Legowo, "Safe avoidance path detection using multi sensor integration for small unmanned aerial vehicle," 2018.

[9] Y. Zeng, F. Zhao, G. Wang, L. Zhang, and B. Xu, "Brain-inspired obstacle detection based on the biological visual pathway," vol. 9919 LNAI, 2016.

[10] C. Häne, L. Heng, G. H. Lee, F. Fraundorfer, P. Furgale, T. Sattler, and M. Pollefeys, "3d visual perception for self-driving cars using a multi-camera system: Calibration, mapping, localization, and obstacle detection," *Image and Vision Computing*, vol. 68, 2017.

[11] B. Singh and M. Kapoor, "A framework for the generation of obstacle data for the study of obstacle detection by ultrasonic sensors," *IEEE Sensors Journal*, vol. 21, 2021.

[12] L. Díaz-Vilariño, P. Boguslawski, K. Khoshelham, H. Lorenzo, and L. Mahdjoubi, "Indoor navigation from point clouds: 3d modelling and obstacle detection," *The International Archives of the Photogrammetry, Remote Sensing and Spatial Information Sciences*, vol. XLI-B4, 2016.

[13] A. Moffatt, E. Platt, B. Mondragon, A. Kwok, D. Uryeu, and S. Bhandari, "Obstacle detection and avoidance system for small uavs using a lidar," 2020.

[14] G. Kucukyildiz, H. Ocak, S. Karakaya, and O. Sayli, "Design and implementation of a multi sensor based brain computer interface for a robotic wheelchair," *Journal of Intelligent and Robotic Systems: Theory and Applications*, vol. 87, 2017.

[15] R. Qin, X. Zhao, W. Zhu, Q. Yang, B. He, G. Li, and T. Yan, "Multiple receptive field network (mrf-net) for autonomous underwater vehicle fishing net detection using forward-looking sonar images," *Sensors*, vol. 21, 2021.

[16] W. Gao, K. Wang, W. Ding, F. Gao, T. Qin, and S. Shen, "Autonomous aerial robot using dual-fisheye cameras," *Journal of Field Robotics*, vol. 37, 2020.

[17] S. Zahran, A. M. Moussa, A. B. Sesay, and N. El-Sheimy, "A new velocity meter based on hall effect sensors for uav indoor navigation," *IEEE Sensors Journal*, vol. 19, 2019.

[18] T. J. Lee, D. H. Yi, and D. I. D. Cho, "A monocular vision sensor-based obstacle detection algorithm for autonomous robots," *Sensors (Switzerland)*, vol. 16, 2016.

[19] F. Valenti, D. Giaquinto, L. Musto, A. Zinelli, M. Bertozzi, and A. Broggi, "Enabling computer vision-based autonomous navigation for unmanned aerial vehicles in cluttered gps-denied environments," vol. 2018-November, 2018.

[20] M. Achtelik, A. Bachrach, R. He, S. Prentice, and N. Roy, "Stereo vision and laser odometry for autonomous helicopters in gps-denied indoor environments," vol. 7332, 2009.

[21] K. McGuire, G. D. Croon, C. D. Wagter, K. Tuyls, and H. Kappen, "Efficient optical flow and stereo vision for velocity estimation and

obstacle avoidance on an autonomous pocket drone," *IEEE Robotics and Automation Letters*, vol. 2, 2017.

[22] L. Matthies, R. Brockers, Y. Kuwata, and S. Weiss, "Stereo vision-based obstacle avoidance for micro air vehicles using disparity space," 2014.

[23] A. Al-Kaff, Q. Meng, D. Martin, A. D. L. Escalera, and J. M. Armingol, "Monocular vision-based obstacle detection/avoidance for unmanned aerial vehicles," vol. 2016-August. Institute of Electrical and Electronics Engineers Inc., 8 2016, pp. 92–97.

[24] F. Saeedan and S. Roth, "Boosting monocular depth with panoptic segmentation maps."

[25] M. Bechini, M. Lavagna, and P. Lunghi, "Dataset generation and validation for spacecraft pose estimation via monocular images processing," *Acta Astronautica*, vol. 204, 2023.

[26] S. Badrloo, M. Varshosaz, S. Pirasteh, and J. Li, "Image-based obstacle detection methods for the safe navigation of unmanned vehicles: A review," *Remote Sensing*, vol. 14, p. 3824, 8 2022.

[27] K. Huh, J. Park, J. Hwang, and D. Hong, "A stereo vision-based obstacle detection system in vehicles," *Optics and Lasers in Engineering*, vol. 46, 2008.

[28] S. Huh, S. Cho, Y. Jung, and D. H. Shim, "Vision-based sense-and-avoid framework for unmanned aerial vehicles," *IEEE Transactions on Aerospace and Electronic Systems*, vol. 51, 2015.

[29] A. Al-Kaff, F. García, D. Martín, A. de la Escalera, and J. M. Armingol, "Obstacle detection and avoidance system based on monocular camera and size expansion algorithm for uavs," *Sensors (Switzerland)*, vol. 17, 5 2017.

[30] A. S. Mashaly, Y. Wang, and Q. Liu, "Efficient sky segmentation approach for small uav autonomous obstacles avoidance in cluttered environment," vol. 2016-November. Institute of Electrical and Electronics Engineers Inc., 11 2016, pp. 6710–6713.

[31] Y. Lin, F. Gao, T. Qin, W. Gao, T. Liu, W. Wu, Z. Yang, and S. Shen, "Autonomous aerial navigation using monocular visual-inertial fusion," *Journal of Field Robotics*, vol. 35, 2018.

[32] W. G. Aguilar, V. P. Casaliglla, and J. L. Pólit, "Obstacle avoidance based-visual navigation for micro aerial vehicles," *Electronics (Switzerland)*, vol. 6, 2017.

[33] S. Badrloo and M. Varshosaz, "Vision based obstacle detection in uav imaging," vol. 42. International Society for Photogrammetry and Remote Sensing, 8 2017, pp. 21–25.

[34] P. Gharani and H. A. Karimi, "Context-aware obstacle detection for navigation by visually impaired," *Image and Vision Computing*, vol. 64, 2017.

[35] T. Mori and S. Scherer, "First results in detecting and avoiding frontal obstacles from a monocular camera for micro unmanned aerial vehicles," 2013.

[36] D. G. Lowe, "Distinctive image features from scale-invariant keypoints," *International Journal of Computer Vision*, vol. 60, 2004.

[37] V. R. Kumar, S. Milz, C. Witt, M. Simon, K. Amende, J. Petzold, S. Yogamani, and T. Pech, "Near-field depth estimation using monocular fisheye camera: A semi-supervised learning approach using sparse lidar data," *CVPR 2018 workshop*, 2018.

[38] M. Mancini, G. Costante, P. Valigi, and T. A. Ciarfuglia, "J-mod 2 : Joint monocular obstacle detection and depth estimation," *IEEE Robotics and Automation Letters*, vol. 3, 2018.

[39] M. A. Haseeb, J. Guan, D. Ristić, and A. Gräser, "Disnet : A novel method for distance estimation from monocular camera," *10th Planning, Perception and Navigation for Intelligent Vehicles*, 2018.

[40] B. Jia, R. Liu, and M. Zhu, "Real-time obstacle detection with motion features using monocular vision," *Visual Computer*, vol. 31, 2015.

[41] N. Ohnishi and A. Imiya, "Appearance-based navigation and homing for autonomous mobile robot," *Image and Vision Computing*, vol. 31, 2013.

[42] C. C. Tsai, C. W. Chang, and C. W. Tao, "Vision-based obstacle detection for mobile robot in outdoor environment," *Journal of Information Science and Engineering*, vol. 34, 2018.

[43] H. Bay, A. Ess, T. Tuytelaars, and L. V. Gool, "Speeded-up robust features (surf)," *Computer Vision and Image Understanding*, vol. 110, 2008.

[44] S. Savant, "A review on edge detection techniques for image," *Ijcsit.Com*, vol. 5, 2014.

[45] T. Y. Goh, S. N. Basah, H. Yazid, M. J. A. Safar, and F. S. A. Saad, "Performance analysis of image thresholding: Otsu technique," *Measurement: Journal of the International Measurement Confederation*, vol. 114, 2018.

[46] X. Ji, A. Vedaldi, and J. Henriques, "Invariant information clustering for unsupervised image classification and segmentation," vol. 2019-October, 2019.

[47] L. Khrissi, N. E. Akkad, H. Satori, and K. Satori, "Clustering method and sine cosine algorithm for image segmentation," *Evolutionary Intelligence*, vol. 15, 2022.

[48] T. M. Quan, D. G. C. Hildebrand, and W. K. Jeong, "Fusionnet: A deep fully residual convolutional neural network for image segmentation in connectomics," *Frontiers in Computer Science*, vol. 3, 2021.

[49] A. Hartigan and M. A. Wong, "A k-means clustering algorithm," *Journal of the Royal Statistical Society*, vol. 28, 1979.

[50] S. M.AqilBurney and H. Tariq, "K-means cluster analysis for image segmentation," *International Journal of Computer Applications*, vol. 96, 2014.

[51] X. Zheng, Q. Lei, R. Yao, Y. Gong, and Q. Yin, "Image segmentation based on adaptive k-means algorithm," *Eurasip Journal on Image and Video Processing*, vol. 2018, 2018.

[52] A. I. Sarpe, "Image segmentation with clustering k-means andwatershed transform," 2010.

[53] N. Dhanachandra, K. Manglem, and Y. J. Chanu, "Image segmentation using k-means clustering algorithm and subtractive clustering algorithm," vol. 54, 2015.

[54] E. Abdel-Maksoud, M. Elmogy, and R. Al-Awadi, "Brain tumor segmentation based on a hybrid clustering technique," *Egyptian Informatics Journal*, vol. 16, 2015.

[55] L. Khrissi, H. Satori, K. Satori, and N. E. Akkad, "An efficient image clustering technique based on fuzzy c-means and cuckoo search algorithm," *International Journal of Advanced Computer Science and Applications*, vol. 12, 2021.

[56] N. K. Verma, P. Gupta, P. Agrawal, M. Hanmandlu, S. Vasikarla, and Y. Cui, "Medical image segmentation using improved mountain clustering approach," 2009.

[57] J. O. Lee, K. H. Lee, S. H. Park, S. G. Im, and J. Park, "Obstacle avoidance for small uavs using monocular vision," *Aircraft Engineering and Aerospace Technology*, vol. 83, 2011.

[58] M. Rasheed, A. H. Ali, O. Alabdali, S. Shihab, A. Rashid, T. Rashid, and S. H. A. Hamad, "The effectiveness of the finite differences method on physical and medical images based on a heat diffusion equation," vol. 1999, 2021.

[59] Y. S. Younis, A. H. Ali, O. K. S. Alhafidhb, W. B. Yahia, M. B. Alazzam, A. A. Hamad, and Z. Meraf, "Early diagnosis of breast cancer using image processing techniques," *Journal of Nanomaterials*, vol. 2022, 2022.

[60] D. G. Honi, A. H. Ali, Z. A. Abduljabbar, J. Ma, V. O. Nyangaresi, K. A.-A. Mutlaq, and S. M. Umran, "Towards fast edge detection approach for industrial products." IEEE, 12 2022, pp. 239–244.

Muhamad Wafi Abdul Aziz has received B.Eng. degree in Aeronautical Engineering Technology (Professional Piloting) with Honor from Universiti Tun Hussein Onn Malaysia. Besides theoretical knowledge of aviation, he also has received a Private Pilot License for Piper 28 aircraft. Currently, he pursuing Master (M.Eng) mainly in computer vision and specifically in obstacle detection and avoidance of Unmanned Aerial Vehicles (UAV). His research interests include machine learning, deep learning and smart agriculture.

Muhammad Faiz Ramli received his degree in Aircraft Engineering Technology from the Malaysia Institute of Aviation Technology. He pursued his master's in aerospace Mechanics and Avionics from the Institut supérieur de l'aéronautique et de l'espace. He completed his Doctorate Philosophy in Mechanical Engineering specialising in UAV System. Currently, he is working as a researcher and Lecturer in the Department of Aeronautical Engineering, Universiti Tun Hussein Onn Malaysia. His research interests are in UAV system and computer vision.